Nanoscale

PAPER

View Article Online
View Journal | View Issue

Cite this: *Nanoscale*, 2025, **17**, 22927

Effects of static electric field and temperature on the dynamic dielectric responses of mixed oil-based and bilayer-stabilised magnetic fluids

Kinnari Parekh, *[a] Ramesh Upadhyay, [a] Michal Rajňák,[b,c] Bystrík Dolník,[c] Milan Timko [b] and Peter Kopčanský[b]

Received 7th July 2025,
Accepted 3rd September 2025

DOI: 10.1039/d5nr02856f

rsc.li/nanoscale

Magnetic fluids based on non-polar liquids constitute attractive materials exhibiting magnetic field-sensitive dielectric relaxation processes. In this study, we focus on the dielectric response of three magnetic fluids with different bilayer stabilisation. The first stabilising layer is a fatty acid, while the second layer is polymeric. The dielectric spectra are studied on thin layers of magnetic fluids in the frequency range from 0.1 Hz to 200 kHz. The presence of the bilayer on the magnetic particle surfaces gives rise to two distinctive relaxation processes observable in permittivity and dissipation factor spectra. We show that the relaxation maxima are significantly sensitive to the acting direct current bias electric voltage (0–3 V). It is found that the bias electric field shifts the relaxation maxima towards higher frequencies and greater permittivity and dissipation factor values. The shift is similar to the effect of temperature, which is also documented in this study. The application of the Havriliak–Negami fitting functions on the studied dielectric spectra is employed in the analysis. The free charge and the resulting conductivity contribution are also taken into account. The direct current-sensitive dielectric response of magnetic fluids may find applications in multifunctional sensors that detect both electric and magnetic fields.

1 Introduction

The stability of magnetic fluids over a long period is affected by many factors, such as (i) the concentration of particles, (ii) particle size and its distribution, (iii) the carrier liquid in which the dispersion of particles is made, (iv) the nature of the surfactant and its compatibility with the surrounding carrier liquid molecules, and (v) external forces such as temperature, gradient magnetic fields, electric fields, *etc*. It is reported in the literature[1–4] that the oversized particles in the system lead to the aggregation and hence affect the stability of the fluid, even if their percentage is tiny. However, the fluid remains stable over time if its presence can be reduced. For some niche applications of magnetic fluids, a specific combination of fluid properties is often required, such as a magnetic fluid-based rotating shaft seal. A rotary seal using magnetic fluid as one element to overcome the effect of pressure differential under a harsh environment, like high speed, high pressure differential, or high torque transmission, demands a special type of magnetic fluid that remains stable under these proposed conditions. In such cases, the evaporation of carrier liquid and the phase separation under prolonged high-speed or high-pressure gradients should be minimal or negligible. To achieve this, very low carrier vapour pressure must be selected; however, with such a type of carrier selection, the viscosity and thermal conductivity change drastically. Therefore, a combination of two carriers is often prepared to optimise the liquid's physicochemical nature.

When a mixture of carrier liquids is prepared, the requirement of a compatible surfactant changes. In such cases, multiple surfactants or layers of surfactants having either the same type or different types must be used to achieve magnetic fluid stability. The choice of surfactant is decided based on the combination of carrier liquids. In our earlier study,[1] an effort was made to prepare three different fluids using two surfactants and two carrier liquids. The physicochemical properties of such fluids have been investigated using XRD, TGA/DSC, FTIR, VSM, and a magneto rheometer. The study confirmed that all three fluids have identical particle sizes, size distributions, and concentrations, but variable surfactant natures and chain lengths. The different hydrodynamic diameters of the particles have altered the fluids' macroscopic magnetic and rheological properties. The ratio of viscous to magnetic torque signifi-

[a]*K C Patel R & D Center, Charotar University of Science & Technology, CHARUSAT Campus, Changa, 388 421, Dist. Anand, Gujarat, India. E-mail: kinnariparekh.rnd@charusat.ac.in*
[b]*Institute of Experimental Physics SAS, Watsonova 47, 04001 Košice, Slovakia*
[c]*Faculty of Electrical Engineering and Informatics, Technical University of Košice, Letná 9, 04200 Košice, Slovakia*

cantly affects the magneto-viscous properties due to the varied nature of the secondary surfactant. This has intrigued us to investigate these fluids for various purposes, such as their dielectric performance under different conditions, such as temperature, DC bias fields, and frequencies. To the authors' knowledge, no such study is reported in the literature.

The dielectric study, conducted between 20 Hz and 2 MHz, on a transformer oil-based magnetic fluid with different volume fractions, showed a maximum shift towards higher frequencies with increasing magnetic nanoparticle concentration.[5] They conclude that the highest dielectric loss observed at around 50 Hz limits the possible use of such magnetic fluids in high-voltage power transformers. In contrast, low dielectric losses at around 2 MHz frequency suggest its possible reliable utilisation in pulsed power system insulation. A dielectric study on transformer oil-based magnetic fluids with different concentrations was performed as a function of frequency from 1 mHz to 200 kHz, and no extra peak at low frequencies was observed.[6] The same author group[7] has reported electrode polarisation and an unusual magnetodielectric effect in a transformer oil-based magnetite magnetic fluid. They explain the observed behaviour due to space charge in the transformer oil due to impurity ions, residual surfactant, and uncompensated particle surface charge. A shift towards low frequencies of dissipation factor upon influence of the electric field on the transformer oil-based magnetic fluid is observed,[8] which is correlated with the transfer of counter ions within a given arrangement. In contrast, it was explained in terms of magnetic fields resulting from the particle aggregation effect. The temperature effect in the range of 15–33 °C was also investigated in the magneto-dielectric study of a transformer oil-based magnetic fluid,[9] in which the value of the dissipation factor increases (at 100 Hz) or decreases (at 7 Hz) with increasing temperature without any changes in the character of its development.

Additionally, several studies have focused on magnetic fluids prepared in different non-aqueous carriers, such as kerosene,[10–13] as a function of frequency and temperature. They reported the appearance of an extra peak in the spectra of the sample at a very low frequency. The origin of this frequency was identified to be from the free charge carriers present in the sample, which may be due to the adsorbed ion on the surface or the ions coming from the carrier. Recently, it was shown that ionic charges responsible for conduction can be generated by the dissociation of surface ligands on the nanoparticles. This has been deduced from the investigation of the direct current behaviour of a kerosene-based ferrofluid. Experimental data reveal linear current–voltage (I–V) characteristics.[10] The influence of free ions on the electric response of cells filled with kerosene-based ferrofluids in the low-frequency region was studied by Batalioto *et al.*[14] They described the analysis of the spectra of the real and imaginary parts of the electric impedance of the cell using a simplified version of the Poisson–Nernst–Planck model, in which only the carriers of a given sign are mobile. Indeed, various issues in the electric response of kerosene-containing magnetic particles to an AC electric field were examined using the impedance spectroscopy technique in the low-frequency range. For instance, the effects of different thicknesses and concentrations of magnetic particles have been reported. It was presented that such magnetic fluids are well described by an electrical circuit formed by a series of two parallel resistance–capacitance elements.[15] Moreover, the nonlinear behaviour of the electric impedance of a kerosene-based ferrofluid subjected to an AC electric voltage of amplitude ranging from 10 mV to 3 V in the frequency range 6.3 mHz to 100 kHz was observed.[16] Even a sinusoidal voltage of amplitude as low as 80 mV can give rise to nonlinear effects for a frequency of the applied voltage smaller than 100 mHz. On the other hand, similar effects of nanoparticles on the electrical properties of a base liquid are reported for various nanofluids. For instance, the electrical conductivity of $NiFe_2O_4$ nanofluids in water and ethylene glycol (EG) as base fluids was investigated at different temperatures and nanoparticle concentrations.[17] It was found that at 70 °C, the electrical conductivity of the $NiFe_2O_4$–water nanofluid increased by 1100% within the volume fraction range of 0–1%. For the $NiFe_2O_4$–EG nanofluid, the increase in electrical conductivity was even more significant, reaching 1235% within the same volume fraction range.

Since, in the present case, we have systems with mixed carriers and mixed surfactants, it is an attractive system to investigate its dielectric response, especially at low frequencies and under DC bias fields and temperatures. The present study highlights the effect of frequencies ranging from 0.1 Hz to 200 kHz under temperature variations from 30 °C to 60 °C, with and without DC bias voltages ranging from 0 to 3000 mV.

2 Experimental

2.1 Magnetic fluid samples

Ferrotec, USA, supplied magnetic fluids for the study. In all three fluids, the identical particles and carrier liquid are used, with the particles having a bilayer coating. The first surfactant is a fatty acid, which is also the same in all three samples, and the second surfactant, polymeric, is different in the three samples. The carrier fluid used is a mixture of hydrocarbon and ester oil. The magnetic fluid parameters specified by the manufacturer are given in Table 1 along with the surfactant (δ) thickness retrieved from the previous study.[1] Where the FTIR measurements of all three samples indicated the presence of a

Table 1 Magnetic fluid parameters provided by the manufacturer (saturation magnetisation (M_s), surfactant thickness (δ), and viscosity (η) along with the particle size (diameter, $\langle D_{MAG} \rangle$) obtained from magnetisation)

Ferrotec sample code	Sample code	M_s (Gauss)	δ (nm)	η@25 °C (mPa s)	$\langle D_{MAG} \rangle$ (nm)
NF4328	S1	211	4.47	96	9.4
NF4325	S2	200	3.79	133	9.4
NF4323	S3	198	2.92	81	9.4

carboxyl group and a polymeric surfactant, but the intensity of the peak corresponding to the carboxyl group was higher in the NF 4323 sample as compared to the other two samples, suggesting a tight binding of the primary surfactant and a lower thickness of the secondary surfactant. The TGA results also confirmed that the tightness of the secondary surfactant decreases systematically from the NF 4323 to NF 4328 samples by shifting the first transition peak from 332 °C to 266 °C. The second transition temperature was observed at 372 °C, revealing that the primary surfactant is the same in all three samples.

The studied magnetic fluids exhibit superparamagnetic behaviour, characterised by zero remanence and coercivity, as revealed by magnetisation measurements at 298 K using a vibrating sample magnetometer (Cryogenic Limited). This state is highlighted in the inset of Fig. 1.

2.2 Experimental method

The dielectric measurements were performed using an LCR meter (IM3533 HIOKI) with 0.05% accuracy. The electric field frequencies employed in this study range from 0.1 Hz up to 200 kHz. We have chosen parallel plate capacitors made from glass plates with indium tin oxide (ITO) layers acting as electrode materials. The capacitor gap is 10 μm and its capacity is 27 pF. This capacity value was used as a divider of the sample-filled capacitor capacity to calculate the real dielectric permittivity. Thus, 10 μm-thick layers of the magnetic fluids were subjected to the complex permittivity and dissipation factor measurements under a sinusoidal voltage with a root mean square value of 200 mV. Besides measuring the alternating current (AC) voltage, the dielectric spectra of the samples were also investigated with a superimposed direct current (DC) voltage. The applied DC bias voltage values are 0, 200, 400, 600, 800, 1000, 1500, 2000, 2500, and 3000 mV. In the 10 μm capacitor gap with the applied voltages, one can get electric field intensities of 20, 40, 60, 80, 100, 150, 200, and 300 kV m^{-1}, respectively. Note that the electric field intensities are comparable to those in electrical engineering practice. The measurements were performed at temperatures of 30, 40, 50, and 60 °C by placing the capacitor in a heating laboratory oven with gentle temperature control. We have selected the given temperature range due to the fact that this temperature range is commonly met in electrical equipment (transformers, circuit breakers, switches and capacitors), where the studied ferrofluids may potentially be applied as functional dielectric fluids. On the other hand, with the selected temperature range, one can avoid a possible risk of thermal energy-induced double-layer surfactant deterioration and production of thermal aging products, which could affect the ferrofluid dielectric response. A flow diagram of the experimental setup is shown in Fig. 2.

3. Results and discussion

3.1 Dielectric study at T = 30 °C for 0 bias field

The room temperature dielectric response and real and imaginary permittivity of three fluids are shown in Fig. 3a–c, respectively, for the NF 4323 to NF 4328 fluids under no bias conditions. Fig. 3 shows that the magnitude of real and imaginary permittivity and their nature significantly differ for all three fluids despite having identical magnetic particles (Fe_3O_4 with 9.2 nm size). A plateau in real permittivity is observed for the NF 4323 fluid at low frequencies, whereas sharp diverging behaviour is observed for the NF 4325 and NF 4328 fluids. Also, the magnitude of real and imaginary permittivity increases from the NF 4323 to NF 4328 fluids. A dissipation factor, tan δ, *versus* frequency shows a clear difference in the emergence of the second relaxation peak in the NF 4325 to NF 4328 fluids at low frequency. Also, the position of the first peak shifts slightly towards higher frequencies. For the NF 4323 fluid, only one peak at 18.9 Hz is observed, whereas for the NF 4325 fluid, two peaks, respectively at 0.25 Hz and 16.2 Hz, are observed. However, the peak intensity for the lower frequency cure is much higher than that of the higher frequency curve. For the NF 4328 fluid, one peak is observed at 0.5 Hz and another peak is observed at 25.3 Hz, but both peaks have similar magnitudes.

A simultaneous increase in real and imaginary permittivity at low frequencies indicates a typical effect of electrode polarization, which results from charge accumulation and the formation of interfacial layers at the metal electrode contacts. This electrode polarization exhibits low mobility. In this case,

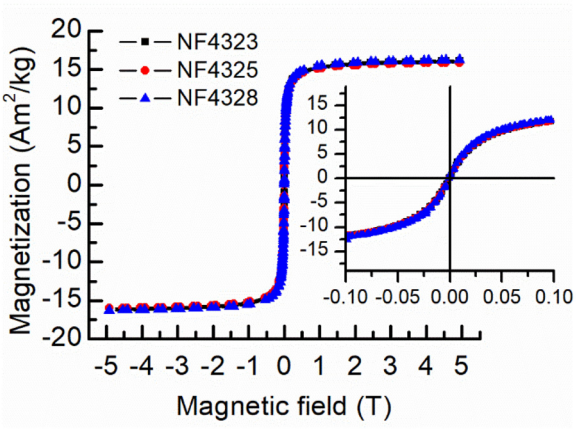

Fig. 1 The studied magnetic fluids' isothermal (298 K) magnetisation curves. The inset shows the superparamagnetic fluctuations of the magnetic moments in the absence of a magnetic field.

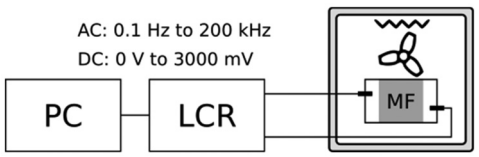

Fig. 2 Flow diagram of the experimental setup consisting of the LCR meter and magnetic fluid (MF) in the plate capacitor placed in a laboratory oven.

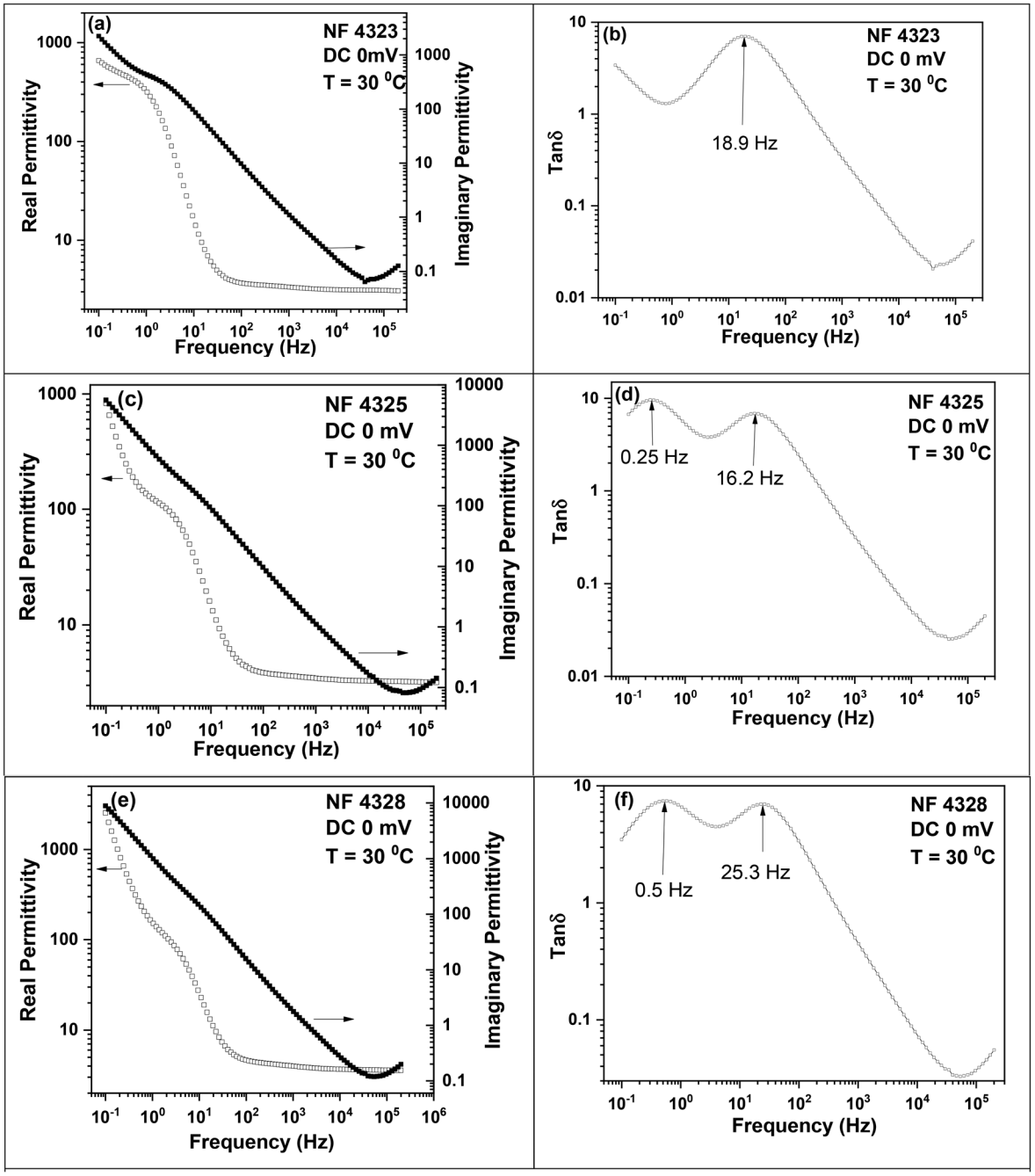

Fig. 3 Real and imaginary permittivities measured at 30 °C under no bias conditions for the (a) NF 4323, (c) NF 4325, and (e) NF 4328 magnetic fluids. Dissipation factor for the (b) NF 4323, (d) NF 4325, and (f) NF 4328 magnetic fluids.

all three fluids demonstrate this behavior at low frequencies. Usually, the characteristic relaxation time is very high, in the MHz range, and the relaxation between 1 and 10 Hz is generally identified as arising from the electric double layer polarization at the nanoparticles' interface. However, this peak shifts towards the 10–30 Hz range in this instance, as all three fluids are concentrated, with a fluid magnetization of ~200 gauss.

In the previous papers,[18–22] the appearance of a low-frequency peak is attributed to the polarisation of an entrapped charge layer near the surface of nanoparticles. This may be due to a free charge adsorbed on the particle surface during the synthesis process or due to the different natures of the surfactant and carrier contributing to the free charges in the system. The dielectric response due to these free charges doesn't follow the fast-changing electric fields, and as a result, its effect diminishes at higher frequencies.

Thus, the appearance of the double relaxation peak in the spectra presented herein reflects two dominating relaxation mechanisms. The fast one, appearing at the higher frequencies, is attributed to the interfacial polarization at the nano-

particle – the first surfactant layer (inner boundary layer). The slow relaxation mechanism at the low-frequency limit is ascribed to the secondary surfactant – carrier liquid polarization. This slow relaxation process is accompanied by the electrode polarization. Both the slow and the fast relaxation processes can be viewed in terms of the well-known Maxwell–Wagner polarization with the related relaxation time $\tau = \varepsilon_0(\varepsilon_1 + \varepsilon_2/\sigma_1 + \sigma_2)$ dependent on permittivities (ε_1 and ε_2) and electrical conductivities (σ_1 and σ_2) of the two interfacial constituents, with ε_0 being the vacuum permittivity. Consideration of the given relaxation time relationship, and taking into account that the electrical conductivity of the nanoparticles is greater than that of the carrier liquid, make it possible to attribute the fast relaxation mechanism to the nanoparticle – first surfactant layer polarization. When the lower electrical conductivities of the secondary surfactant and the carrier liquid are considered, one obtains the greater relaxation time observed in the low-frequency limit.

Additionally, as mentioned above, the surfactant coating is much tighter in the case of the NF 4323 sample compared to the NF 4325 and NF 4328 samples. This may explain why the low-frequency peak for the NF 4323 sample is not observed, whereas it is present for the other two samples. Since the volume fractions of all three fluids are high, many free charges accumulate near the particle surface, making the system very interesting to investigate as a function of temperature and DC electric fields. To better understand the observed results, the data were analyzed using the Havriliak–Negami function.

3.1.1 Evaluation of dielectric spectra using the Havriliak–Negami (H–N) model. The dielectric spectra are typically described using the classical Debye model, represented as:

$$\varepsilon = \varepsilon_\infty + \frac{\Delta\varepsilon}{1 + i\omega\tau}, \tag{1}$$

where $\Delta\varepsilon = \varepsilon_s - \varepsilon$, in which, ε_s is the stationary permittivity at low frequencies, ε_∞ is the limit of permittivity at high frequencies, ω is the angular frequency, and τ is the relaxation time. The Debye model is modified by Havriliak–Negami (H–N),[23] considering the broadening (β) and asymmetry (γ) of the dielectric dispersion curve resulting from a distribution of relaxation times rather than just one. The Havriliak–Negami Model is expressed as follows:

$$\varepsilon = \varepsilon_\infty + \frac{\Delta\varepsilon}{(1 + (i\omega\tau)^\beta)^\gamma} \tag{2}$$

There are conductive processes alongside the relaxation process, which contribute to the dielectric function, especially at the low frequencies. If this is due to a pure electronic origin, then the contribution to the imaginary part of ε is considered as $\sigma_{DC}/\varepsilon_0\omega$. The other contributions can be accounted for by the addition of an exponent $s \leq 1$ in ω as $\sigma_{DC}/\varepsilon_0\omega^s$. The real part of the dielectric permittivity using the Havriliak–Negami equation is then written as:

$$\varepsilon' = \varepsilon_\infty + \Delta\varepsilon \times r(\omega) \times \cos(\gamma\varphi(\omega)) \tag{3}$$

where

$$r(\omega) = \left[1 + 2(\omega\tau)^\beta \cos\left(\frac{\beta\pi}{2}\right) + (\omega\tau)^{2\beta}\right]^{-\gamma/2} \tag{4}$$

and

$$\varphi(\omega) = \arctan\left[\frac{\sin\left(\frac{\beta\pi}{2}\right)}{(\omega\tau)^{-\beta} + \cos\left(\frac{\beta\pi}{2}\right)}\right] \tag{5}$$

β and γ are strongly anti-correlated, obeying the constraint relationship $0 < \beta\,\gamma \leq 1$. Similarly, after incorporating the conductivity term in the H–N equation, the imaginary part of the dielectric constant is expressed as:

$$\varepsilon'' = \Delta\varepsilon \times r(\omega) \times \sin\left(\gamma\varphi(\omega) + \frac{\sigma'}{\omega^s}\right) \tag{6}$$

Similarly, the DC conductivity is strongly correlated with s; both parameters appear only in the additive term.

Since the conductivity term in the H–N fit is dominant at low frequencies, we have deconvoluted the observed dielectric spectrum into two curves. One curve has a peak at low frequencies, while the other peaks at high frequencies. The electronic contribution primarily dominates the first term, whereas the second peak corresponds to the particles' classical Debye nature. We obtained the fitting parameters by fitting the dielectric spectra with the Havriliak–Negami model and the conductivity term. Table 2 presents the H–N fit parameters for all three fluids.

Table 2 shows that the symmetry of the dielectric distribution curve (γ) and the conductivity term (σ') corresponding to peak 1

Table 2 H–N fit parameters for the three magnetic fluids at 30 °C under 0 DC bias voltage

Sample	NF 4323		NF 4325		NF 4328	
Parameters	Peak-1	Peak-2	Peak-1	Peak-2	Peak-1	Peak-2
DC bias (mV)	0	0	0	0	0	0
$\Delta\varepsilon$	411.7	424.4	12 075.0	115.8	21 547	89.2
β	1	1	1	1	1	1
γ	0.846	1	1	0.958	0.9664	0.9863
τ	1.775	0.0980	6.3747	0.0542	4.8851	0.0344
ε_∞	1.605	1.605	1.674	1.676	1.8819	1.8819
s	1	1	1	1	1	1
σ'	623.6	623.6	356.1	1368.2	738.0	738.0

increases from the NF 4323 to NF 4328 samples. This indicates that free charges in the NF 4328 fluid are maximized compared to the other two fluids. The origin of these free charges could stem from the secondary surfactant or the mixed carrier, which polarize differently under the applied electric fields. However, s = 1 in all the samples indicates that the source is due to a pure electronic origin. In the NF 4323 sample, the peak at the low frequency falls beyond the minimum frequency used in the measurement. In contrast, NF 4325 appears initially, while the 4328 sample is observed at a relatively high frequency, which is also reflected in the dissipation factor from Fig. 3(b, d, and f). To our surprise, the fitted value of the relaxation time is the highest for the NF4328 fluid and the lowest for the NF4323 fluid. Thus, the relaxation time correlates with the number of free charge carriers. We have experimented with various biasing voltages and temperatures to gain a deeper understanding of this phenomenon.

3.2 Dielectric spectrum: DC bias field dependent (bias field = 0–3000 mV)

The effect of the DC bias voltage ranging from 0 to 3000 mV on both real and imaginary permittivity, as well as the dissipation factor at 30 °C, was investigated for all three fluids. Fig. 4 (a–c) illustrate the variation in real permittivity for the NF 4323, NF 4325 and NF 4328 magnetic fluids, respectively. Two notable features are observed in Fig. 4: (i) the dielectric dispersion shifts significantly towards higher frequencies with increasing bias voltage at 30 °C and (ii) the low-frequency permittivity rises as the bias voltage increases. However, the imaginary permittivity spectra as observed in Fig. 4(d–f) do not exhibit distinct bifurcations with increasing bias voltage, despite an increase in magnitude for all three fluids. Fig. 4 (g–i) depicts the dissipation factor as a function of frequency under the DC bias voltage from 0 to 3000 mV at 30 °C for all three fluids, respectively. The dissipation factor value increases at low frequencies as the bias voltage rises. The increase in real permittivity at low frequencies with the increasing bias voltage can be attributed to the fact that the applied DC voltage induces cluster formation of nanoparticles driven by the magnitude of the DC bias. This type of cluster formation under the DC bias voltage is also observed in other magnetic fluids based on transformer oil.[8]

For the NF 4325 fluid, two clear relaxation peaks are evident for this fluid in the real permittivity spectrum. Despite the increasing magnitude, the imaginary permittivity spectra do not exhibit very distinct bifurcations as the bias voltage rises. The dissipation factor increases at low frequencies with

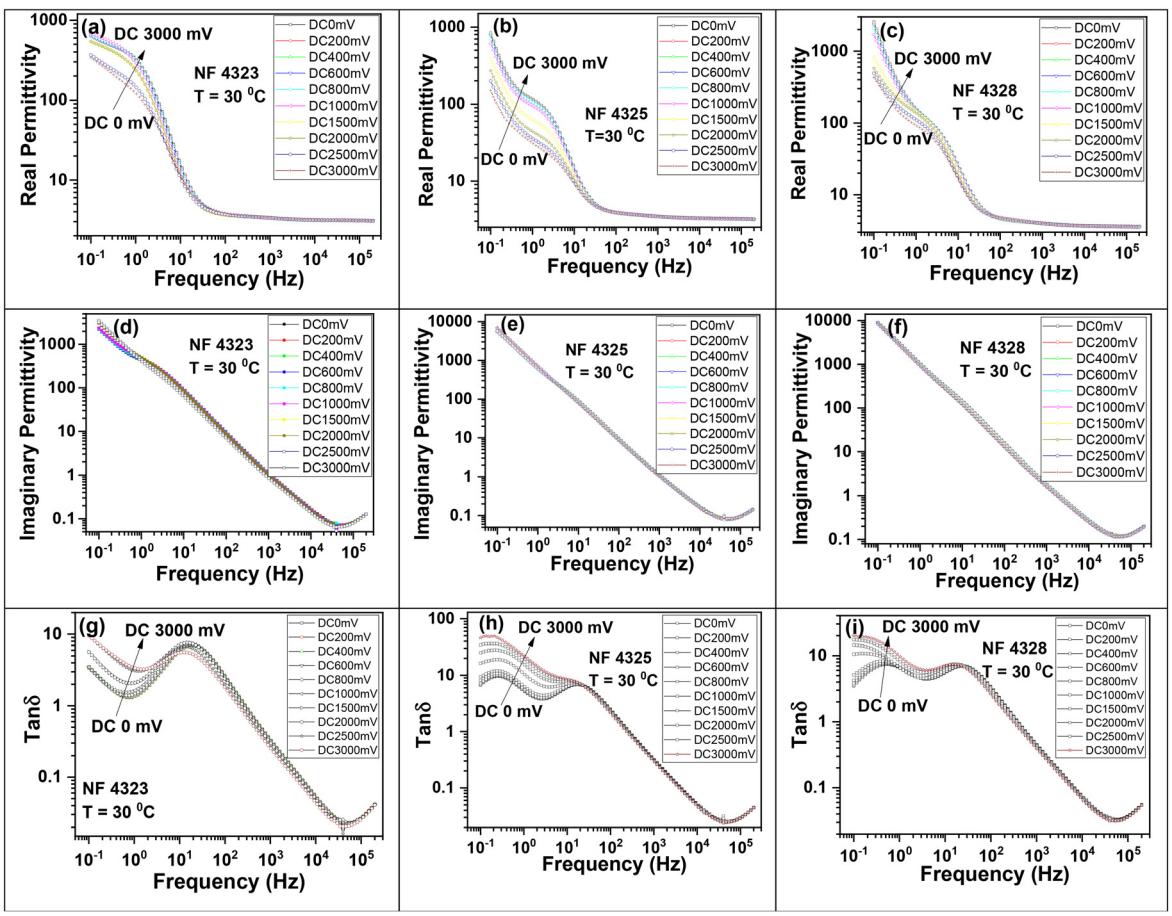

Fig. 4 Real permittivity (a)–(c), imaginary permittivity (d)–(f), and dissipation factor (g)–(i) as a function of frequency under different bias conditions at 30 °C for the NF 4323 magnetic fluid, NF 4325 magnetic fluid, and NF 4328 magnetic fluid, respectively.

increasing bias voltage, and its magnitude is also the highest in this sample compared to the other two fluids. For the NF 4328 fluid, the DC bias voltage from 0 to 3000 mV showed a similar effect in real permittivity with two clear relaxation peaks which are positioned at higher frequencies than the above two fluids. The higher value of the real permittivity spectrum in both the NF 4325 and NF 4328 fluids indicates the liberation of free charges upon application of DC bias fields, the effect of which can be further analysed using the H–N fit, as shown in below section.

3.2.1 H–N fit to samples under different DC biases. The permittivity spectra of the NF 4323, NF 4325, and NF 4328 samples were fitted with the H–N equation at 30 °C for different bias voltages ranging from 0 to 3000 mV. The relaxation times for the first and second peaks in all three fluids show a variation under biasing voltages, as illustrated in Fig. 5a and b. Nevertheless, the value of τ_2 is two orders of magnitude less than that of τ_1. The τ_2 value remains almost constant up to approximately 1000 mV, and thereafter it exhibits a slight change in its value for all three fluids. However, this change is minimal, indicating a pure Debye relaxation of the particles. For the NF 4323 fluid, the τ_1 value decreases with increasing DC bias voltage, whereas it increases for the other two fluids. The decrease in relaxation time indicates a reduction in the first peak due to the biasing field. In contrast, for the NF 4325 and NF 4328 fluids, the increase in the τ_1 value suggests the accumulation of charge carriers under the influence of DC bias fields. This behavior may be attributed to the liberation of charge upon the application of DC bias voltage, resulting in increased conductivity. The origin of the free charges may lie in the secondary surfactant, as observed in the analysis of magnetorheology results, where the thickness of the surfactant is the highest (almost double than that in the NF 4323 fluid) in the NF 4328 fluid compared to the NF 4325 and NF 4323 fluids.[1] Simultaneously, the TGA data indicate that the secondary surfactant is coiled up in the NF 4328 fluid. We suspect that the opening of the tail of a secondary surfactant upon the application of DC bias voltage contributes to the conductivity.

The variation of $\Delta\varepsilon_1$ and $\Delta\varepsilon_2$ values as a function of DC bias voltage is evident from Fig. 5c and d, respectively. The magnitude of $\Delta\varepsilon_1$ is two orders of magnitude greater than that of $\Delta\varepsilon_2$, indicating that the contribution of the first peak is substantially higher than that of the second peak. Furthermore, the $\Delta\varepsilon_2$ value remains constant up to 800 mV for all three fluids and then decreases after 800 mV for the NF 4323 and NF 4325 fluids, while it remains nearly constant for the NF 4328 fluid. This behavior may be related to the classical Debye-like nature of permittivity. It is observed that the value of $\Delta\varepsilon_1$ remains the same for the NF 4323 fluid, while for the NF 4328

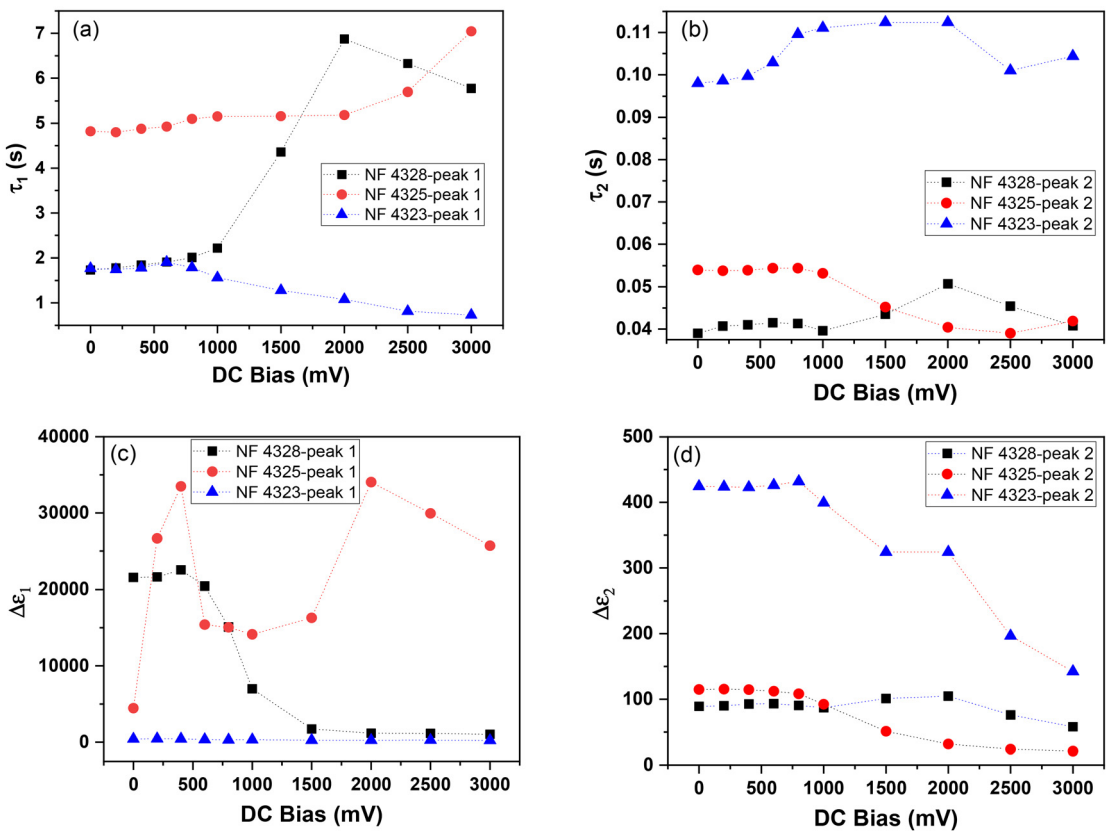

Fig. 5 Relaxation time for (a) the low-frequency peak and (b) the high-frequency peak and variation in (c) the $\Delta\varepsilon_1$ and (d) $\Delta\varepsilon_2$ values as a function of DC bias voltages for all three samples.

fluid, it remains constant up to 800 mV and then decreases afterwards. For the NF 4325 fluid, the $\Delta\varepsilon_1$ value increases significantly with slight applied bias voltage, decreases to a plateau, and then increases again. The variation in the $\Delta\varepsilon_1$ value suggests that the difference between the initial and infinite permittivities either increases or decreases as the bias voltage rises. This may be linked to the binding strength of the secondary surfactant on the primary surfactant-coated particles in the NF 4325 sample. The constant value of $\Delta\varepsilon_1$ for the NF 4323 fluid indicates that the DC bias field does not influence the liberation of free charges from the surfactant, maintaining a constant permittivity value upon the application of DC bias fields. In contrast, for $\Delta\varepsilon_2$, the permittivity value decreases above the 800 mV bias field, suggesting that Debye relaxation is affected beyond the mentioned DC bias fields.

Fig. 6a and b illustrate the variation in γ values for peaks 1 and 2 as a function of DC bias voltage at 30 °C. The value of γ represents the asymmetry of the dielectric dispersion curve; if it remains constant, it indicates a symmetric distribution of the curve, while a decreasing value suggests that the dielectric dispersion alters the nature of the distribution curve. For the NF 4328 fluid, the γ value for peak 1 decreases significantly after 800 mV and levels off, whereas for peak 2 it remains almost constant between 0.98 and 1. In contrast, for the NF 4325 fluid, peak 1 slightly decreases and then stabilizes, while peak 2 declines sharply from 0.96 to 0.81. For the NF 4323 fluid, the γ value increases for peak 1, while it remains constant for peak 2 up to 2000 mV, before decreasing to 0.92.

As seen from Fig. 6c, the conductivity in all the fluids increases with the DC bias voltages. Initially, the increase in conductivity is minimal up to 500 mV, but between 500 mV and 1500 mV, the increase is significantly high and non-monotonic; afterwards, the conductivity reaches saturation for all three fluids. Among the three fluids, this value is significantly high in NF 4328, indicating that the number of free charge carriers in the samples increases rapidly with the bias voltage in the NF 4328 fluid compared to the NF 4325 fluid. For the NF 4323 fluid, this change is minimal, even though the bias voltage influences it.

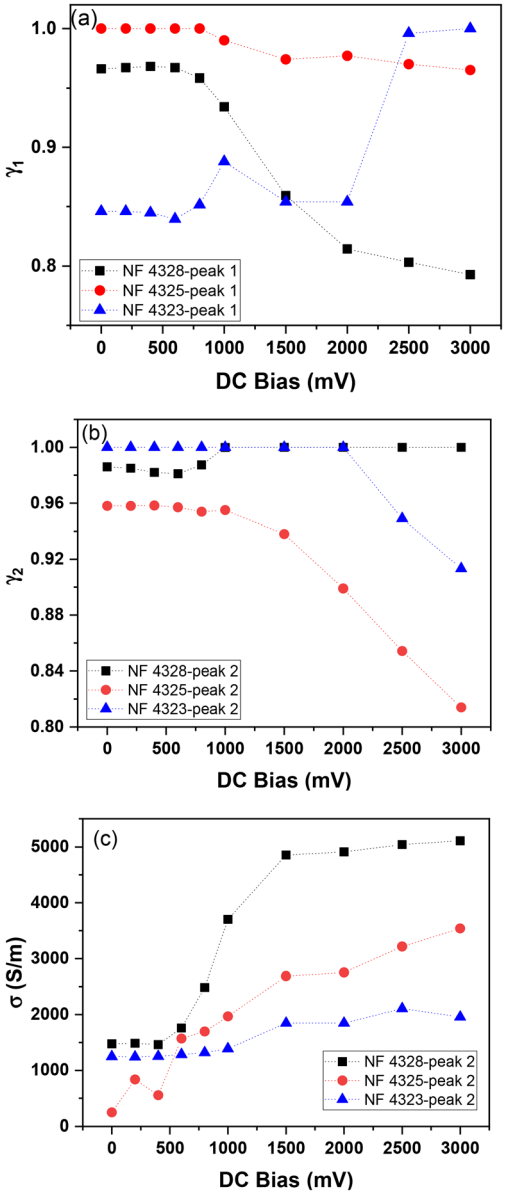

Fig. 6 Variation in the (a) γ_1 and (b) γ_2 values and (c) conductivity as a function of DC bias voltages for all three samples.

3.3 Effect of temperatures

Fig. 7 illustrates the effect of temperatures ranging from 30 °C to 60 °C, measured at 10 °C intervals, for the NF 4323 fluid under 0 bias conditions. As shown in Fig. 7a, the low-frequency real permittivity sharply increases as the temperature rises, while the initial plateau region decreases. This unusual behavior suggests that the contribution from free charges in the system may increase with increasing temperature. The imaginary permittivity, as indicated in Fig. 7d, remains relatively unchanged. However, the loss factor introduces a low-frequency peak with increasing temperature, as seen in Fig. 7g.

Similar behavior is observed in the NF 4325 sample regarding the real permittivity, as illustrated in Fig. 7b, where the low-frequency real permittivity increases sharply with rising temperature, and the initial plateau region diminishes. However, compared to the NF 4323 fluid, the diverging behavior at low frequency is two orders of magnitude higher. The imaginary permittivity depicted in Fig. 7e does not significantly change with temperature variations. Nevertheless, the loss factor demonstrates a systematic shift of the low-frequency peak towards higher frequencies with increasing temperature, as shown in Fig. 7h. The NF 4328 fluid also behaves similarly to the NF 4325 fluid under 0 bias conditions with increasing temperatures (Fig. 7c, f, and i).

The dielectric spectra show that the fast relaxation process (nanoparticle – first surfactant layer) is more sensitive to temperature, as the related maximum shifts towards higher frequencies in a greater measure as compared with the DC bias effect. The remarkable temperature effect on the fast relaxation process is associated with the temperature-

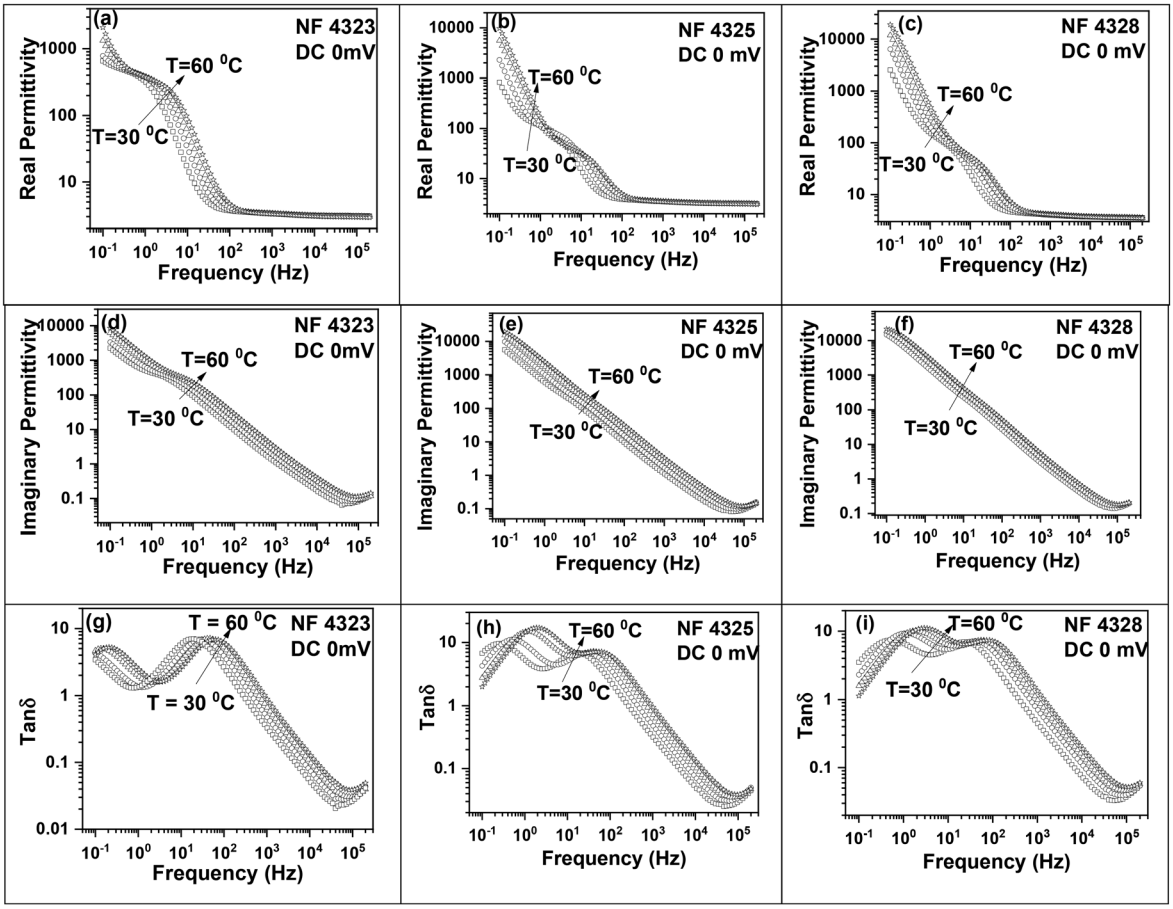

Fig. 7 Real permittivity (a)–(c), imaginary permittivity (d)–(f), and dissipation factor (g)–(i) as a function of frequency under 0 bias conditions for the NF 4323, NF 4325, and NF 4328 magnetic fluids, respectively.

dependent electrical conductivity of the nanoparticles. The increasing temperature causes an increase in the nanoparticles' electrical conductivity and it results in a decrease in the relaxation time.

A detailed study of all three samples with different DC bias voltages has also been conducted, and the results have been analysed using the H–N fit. The analysis is shown in Fig. 8 for all three fluids. It is seen from the figure that the value of $\Delta\varepsilon_1$ is almost two orders of magnitude higher than that of $\Delta\varepsilon_2$, irrespective of the type of fluid. $\Delta\varepsilon_1$ is the difference between the infinite permittivity and the lowest permittivity. The higher value indicates the strength of peak 1, which dominates all three fluids, indicating that the contribution of peak 1 is much higher than that of peak 2. This contribution further increases with an increase in the temperature for both $\Delta\varepsilon_1$ and $\Delta\varepsilon_2$. However, the increase in the magnitude of $\Delta\varepsilon_2$ is slight for all three fluids and may be correlated with the increasing diffusion of particles in the medium due to their higher kinetic energy.

The $\Delta\varepsilon_1$ value for the NF 4323 fluid showed a drastic increase above 50 °C and 60 °C, even under 0 bias conditions, indicating that the free charge carriers are liberated from the secondary surfactant upon increasing the temperature. In the case of the NF 4325 fluid, the $\Delta\varepsilon_1$ value increases initially from 30 °C to 40 °C and remains the same for higher temperatures under zero bias conditions, whereas for the NF 4328 fluid, the $\Delta\varepsilon_1$ value increases with increasing temperature.

With the influence of the DC bias voltage, it is observed that the value of $\Delta\varepsilon_1$ initially increases, reaching a peak at 500 mV, and then begins to decrease with increasing bias voltages. This behaviour is identical for all three fluids at every temperature except for the NF4325 fluid at 30 °C. The deviation in the NF 4325 fluid at 30 °C may be correlated to the fluid's viscosity, since the particle size and concentration is the same for all three fluids. The first surfactant layer is also identical for the three fluids, only secondary surfactant differs in its composition and thickness. This causes a remarkable difference in the viscosity of the fluid, which is very high at 135 mPa s for the NF 4325 fluid as compared to the other two fluids, hindering the diffusion of charge carriers and magnetic particles in the medium. However, with slightly higher temperatures, the fluid's viscosity reduces, and the expected behaviour is observed. In the case of $\Delta\varepsilon_2$, it remains constant up to 1000 mV and then starts decreasing.

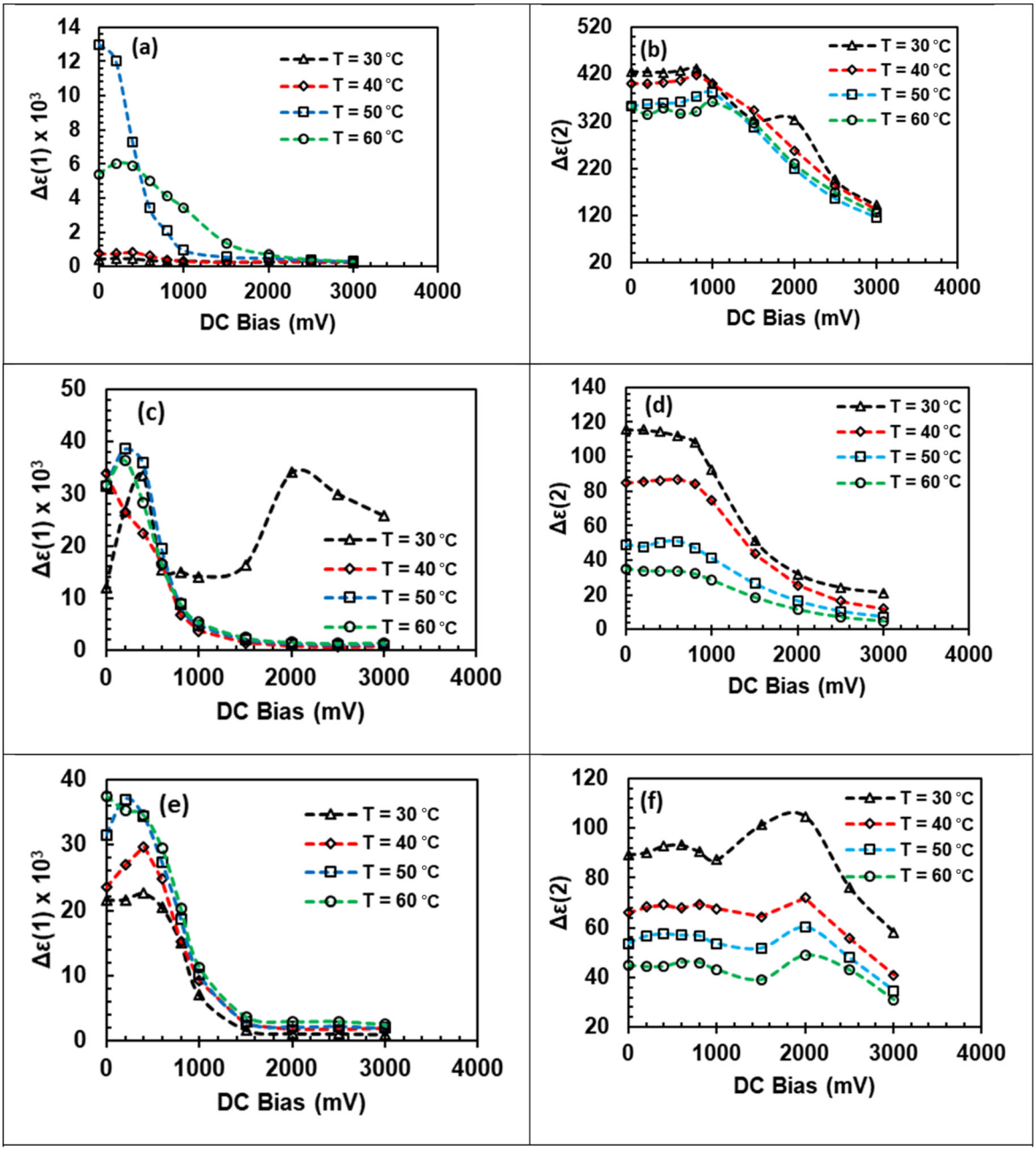

Fig. 8 $\Delta\varepsilon_1$ values for the (a) NF 4323 fluid, (c) NF 4325 fluid, and (e) NF 4328 and $\Delta\varepsilon_2$ values for the (b) NF 4323 fluid, (d) NF 4325 fluid, and (f) NF 4328 fluid as a function of DC bias voltages.

Fig. 9 shows the variation in relaxation time (both τ_1 and τ_2) as a function of DC bias voltages for 30 °C, 40 °C, 50 °C, and 60 °C temperatures for all three fluids. The relaxation time observed for peak 1 is two orders of magnitude higher than that for peak 2, irrespective of the nature of the sample. However, τ_1 reduces faster with DC bias voltages, whereas τ_2 shows a negligible variation with the DC bias. Also, the relaxation time (both τ_1 and τ_2) increases with an increase in the temperature from 30 °C to 60 °C, except for the NF 4323 sample, where the value of τ_1 decreases at 60 °C to that observed at 50 °C. The reason for this observed decrease is unknown to us. For the NF 4325 sample, the value of τ_1 at 60 °C decreases initially and then increases drastically.

Fig. 10 illustrates the conductivity behavior as a function of DC bias voltage for the three fluids. The conductivity remains nearly constant up to 750 mV DC bias. In contrast, a non-monotonic increase is observed when the DC bias is between 750 mV and 2000 mV, and then, at higher DC bias levels, it reaches saturation. This pattern holds true for all temperatures and all types of fluids under investigation. However, the value

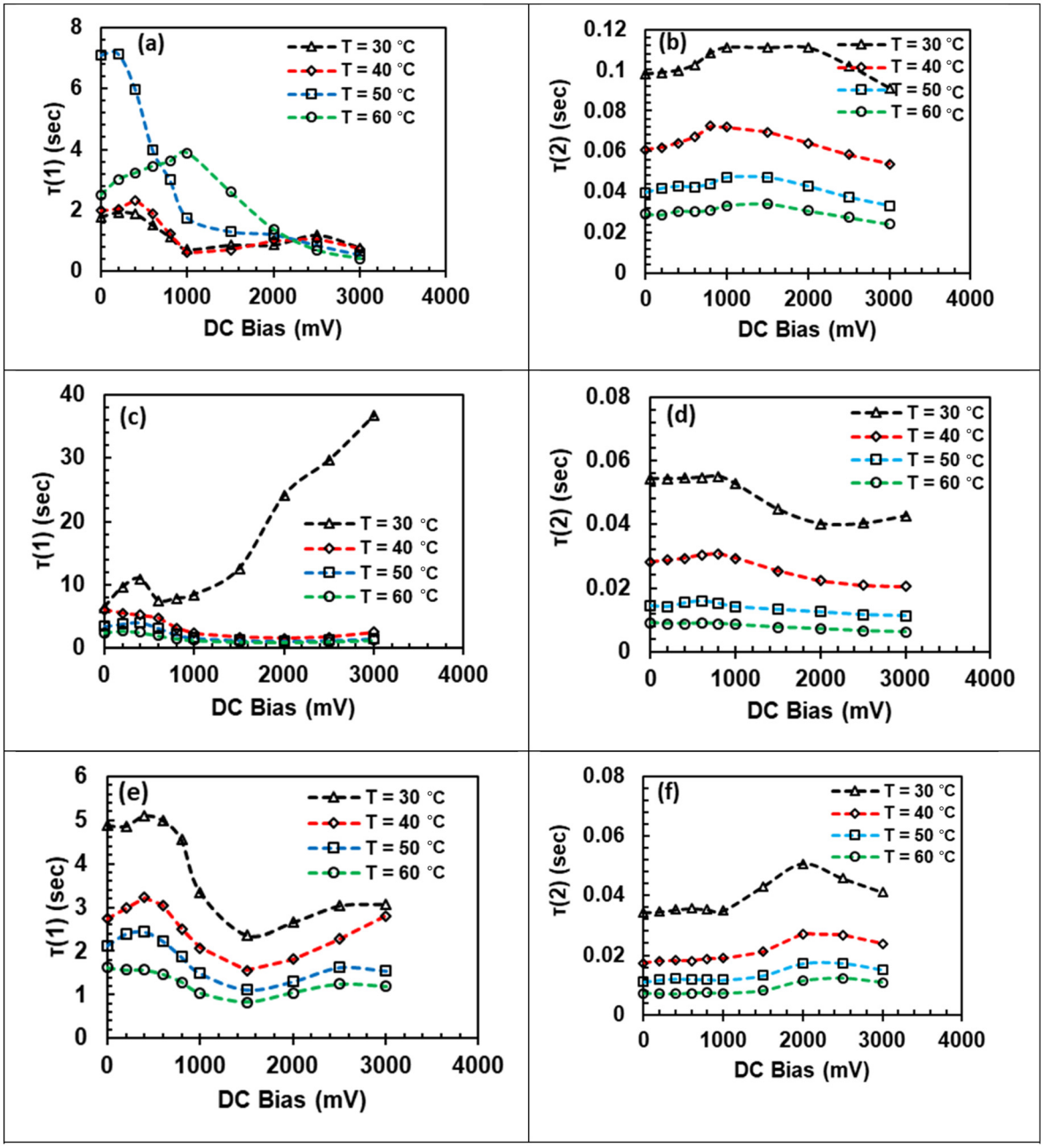

Fig. 9 Relaxation time as a function of DC bias voltages for peak 1: (a) NF 4323 fluid, (c) NF 4325 fluid, and (e) NF 4328 fluid and for peak 2: (b) NF 4323 fluid, (d) NF 4325 fluid, and (f) NF 4328 fluid.

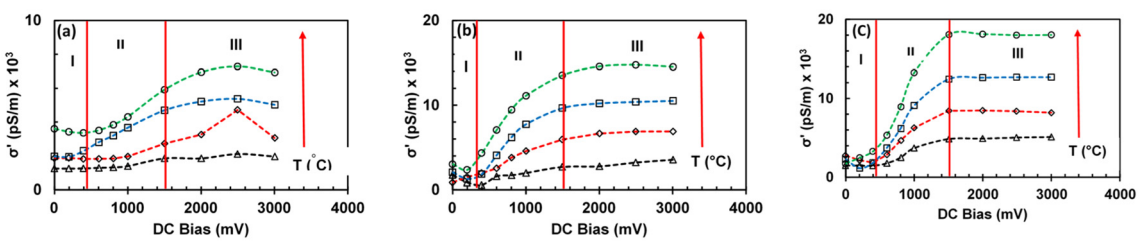

Fig. 10 Variation in conductivity as a function of DC bias voltages for the (a) NF 4323 fluid, (b) NF 4325 fluid, and (c) NF 4328 fluid.

is relatively low for the NF 4323 fluid compared to the other two fluids, which aligns with the expected results, as the number of free charges is lower in this particular sample.

In summary, we conclude that the nature and types of secondary surfactant in the sample influence the dielectric response of the magnetic fluid significantly at low frequency since the particle composition, particle size, size distribution, primary surfactant and dispersion medium are identical. The low frequency behavior changes significantly upon increasing the temperature or DC bias fields.

4 Conclusion

The current experimental investigations elucidate the contribution of the secondary surfactant to the low-frequency dielectric spectra of three colloids. A plateau in real permittivity is observed for the NF 4323 fluid at low frequencies, whereas the NF 4325 and NF 4328 fluids show a sharp diverging behavior with increased magnitudes of real and imaginary permittivity. The dissipation factor, $\tan\delta$, *versus* frequency reveals a clear difference in the emergence of the second relaxation peak between the NF 4325 and NF 4328 fluids at low frequencies. The results were analyzed using the HN fit, which indicates a higher value of the conductivity term corresponding to peak 1, increasing from the NF 4323 to NF 4328 samples. This suggests that free charges in the NF 4328 fluid are maximized compared to the other two fluids. The appearance of the low-frequency peak correlates with the presence of free charges that may originate from the secondary surfactant.

The fluids studied present an exciting opportunity to understand the origin of free charges in the system and their behavior at various temperatures and DC bias fields. The low frequency peak appears in the sample when free charges are present, and its dominance increases with the strength of the free charges—the peak intensity increases as temperature or the applied DC bias field increases. The relaxation time corresponding to the low frequency peak changes drastically with the application of the DC bias field and temperature.

The application of DC bias field affects the liberation of free charges from the secondary surfactant, resulting in changes in the value of $\Delta\varepsilon_1$. The results show that the $\Delta\varepsilon_1$ value remains the same for the NF 4323 fluid, whereas for the NF 4328 fluid, it remains constant up to 800 mV and then decreases. For the NF 4325 fluid, the $\Delta\varepsilon_1$ value increases drastically under a small applied biasing voltage, decreases to a plateau, and increases again. The increasing or decreasing value indicates that the difference between the initial and infinite permittivities either increases or decreases with the increase in bias voltage. This may be correlated with the binding strength of the secondary surfactant on primary surfactant-coated particles in the NF 4325 sample.

With increasing temperature, it increases; however, with increasing DC bias fields, the relaxation time decreases and eventually becomes constant. Above a specific critical value of DC bias fields, the contribution from free charges remains constant and is independent of the sample or temperature. In this case, this value is 1500 mV. Thus, the study explains the low-frequency dielectric behavior in magnetic fluids with different secondary surfactants.

Author contributions

KP – methodology, investigation, data curation, data analysis, validation, visualization, resources, and writing the first draft of the manuscript; MR – measurements of magnetic properties and dielectric spectroscopy, data curation, and analysis; BD – measurements of dielectric spectroscopy, software, data curation, and analysis; MT – validation; PK – validation and resources; RU – methodology, data analysis, validation, and visualization. All authors have gone through the final draft of manuscript.

Conflicts of interest

The authors disclose no financial or non-financial interests directly or indirectly related to the work submitted for publication.

Data availability

Data available on request from the authors.

Acknowledgements

The authors thank Ferrotec, USA, for providing the samples for this study. We also acknowledge the financial support from Charotar University of Science and Technology for the research. Part of this research was funded by the Slovak Research and Development Agency under Contract No. APVV-22-0115 and APVV-22-0060, as well as the Slovak Academy of Sciences and the Ministry of Education within the framework of Projects VEGA No. 2/0029/24, 1/0627/24, 2/0028/25, and 2/0061/24 and the Cultural and Educational Grant Agency of the Ministry of Education, Research, Development and Youth of the Slovak Republic under Contract No. 008TUKE-4/2019. The work also received support from REA.A – Marie Skłodowska Curie Actions & Support to Experts within Project No. 101182948—RETROTRAFO—HORIZON-MSCA2023-SE-01.

References

1 R. V. Upadhyay, K. Raj, K. H. Parekh and M. S. Pisuwala, *Chem. Pap.*, 2023, 77, 2871.
2 S. Odenbach and S. Thurm, Magneto-viscous Effects in Ferrofluids, in *Ferrofluids, Lecture Notes in Physics*, ed. S. Odenbach, Springer, Berlin, 2002.

3 R. E. Rosensweig, *Ferrohydrodynamics*, Cambridge University Press, Cambridge, 1985.
4 L. Vekas, D. Bica and O. Marinica, Magnetic nanofluids stabilized with various chain length surfactants, *Rom. Rep. Phys.*, 2006, **58**, 257–267.
5 M. Rajnak, J. Kurimsky, B. Dolnik, K. Marton, L. Tomco, A. Taculescu, L. Vekas, J. Kovac, I. Vavra, J. Tothova, P. Kopcansky and M. Timko, *J. Appl. Phys.*, 2013, **114**, 034313.
6 M. Rajňák, B. Dolník, K. Paulovičová, R. Cimbala, P. Kopčanský, M. Timko, K. Parekh and R. V. Upadhyay, *J. Chem. Phys.*, 2023, **158**, 204901.
7 M. Rajnak, B. Dolnik, J. Kurimsky, R. Cimbala, P. Kopcansky and M. Timko, *J. Chem. Phys.*, 2017, **146**, 014704.
8 Š. Hardon, J. Kúdelcík, P. Bury and M. Gutten, *Acta Phys. Pol., A*, 2018, **133**(3), 477.
9 J. Kúdelcík, Š. Hardon, P. Bury, M. Timko and P. Kopcanský, *Acta Phys. Pol., A*, 2018, **133**(3), 483.
10 B. M. Oliveira, F. Batalioto, M. Chand, A. F. C. Campos, G. Barbero and A. M. Figueiredo Neto, *J. Appl. Phys.*, 2025, **137**, 134701.
11 A. M. Antonova, G. Barbero, F. Batalioto, A. M. Figueiredo Neto and K. Parekh, *J. Electroanal. Chem.*, 2020, **856**, 113479.
12 I. Malaescu1 and C. N. Marin, *J. Colloid Interface Sci.*, 2002, **251**, 73.
13 M. M. Radulescu, *J. Magn. Magn. Mater.*, 1990, **85**, 144.
14 F. Batalioto, G. Barbero, A. F. C. Campos and A. M. Figueiredo Neto, *Phys. Chem. Chem. Phys.*, 2021, **23**(4), 2819.
15 F. Batalioto, E. S. Gonçalves, A. M. F. Neto and G. Barbero, *J. Electroanal. Chem.*, 2020, **874**, 114452.
16 F. Batalioto, M. Chand, A. F. C. Campos, J. Depeyrot, G. Barbero and A. M. F. Neto, *Phys. Chem. Chem. Phys.*, 2022, **24**(46), 28506.
17 M. Dolati, H. Khandan Fadafan and M. Abareshi, *Nano-Struct. Nano-Objects*, 2024, **39**, 101266.
18 I. Malaescu and C. N. Marin, *J. Magn. Magn. Mater.*, 2002, **252**, 68.
19 I. Malaescu and C. N. Marin, *J. Colloid Interface Sci.*, 2002, **251**, 73.
20 M. Rajnak, B. Dolnik, J. Krempasky, R. Cimbala, K. Parekh, R. Upadhyay, K. Paulovicova, P. Kopcansky and M. Timko, *J. Phys. D:Appl. Phys.*, 2020, **54**, 035303.
21 M. Rajnak, J. Kurimsky, B. Dolnik, P. Kopcansky, N. Tomasovicova, E. A. Taculescu-Moaca and M. Timko, *Phys. Rev. E:Stat., Nonlinear, Soft Matter Phys.*, 2014, **90**, 032310.
22 M. Rajnak, J. Kurimsky, B. Dolnik, K. Marton, L. Tomco, A. Taculescu, L. Vekas, J. Kovac, I. Vavra, J. Tothova, P. Kopcansky and M. Timko, *J. Appl. Phys.*, 2013, **114**, 034313.
23 S. Havriliak and S. Negami, *Polymer*, 1967, **8**, 161.